

Multiple-scattering Optical Tomography with Layered Material

Toru Tamaki, Bingzhi Yuan, Bisser Raychev, Kazufumi Kaneda
Graduate School of Engineering, Hiroshima University, Japan
tamaki@hiroshima-u.ac.jp

Yasuhiro Mukaigawa
ISIR, Osaka University, Japan
mukaigaw@am.sanken.osaka-u.ac.jp

Abstract—In this paper, we propose an optical tomography for optically dense media in which multiple scattering is dominant. We model a material by many layers of voxels, and light scattering as a distribution from a voxel in one layer to other voxels in the next layer. Then we write attenuation of light along a light path by an inner product of vectors, and formulate the scattering tomography as an inequality constraint minimization problem solved by interior point methods. We show experimental results with numerical simulation for evaluating the proposed method.

Keywords—scattering of light, optical tomography, scattering tomography, inverse scattering, inequality constraint optimization

I. INTRODUCTION

Tomography, an inverse problem to see inside materials by observing output of a structured input, is an important issue in physics, medical imaging, computer vision and related research field [1]–[7]. A well known application widely used for medical purpose is Computed Tomography (CT) with X-ray [8]. The property of penetrating a body enable us to observe the X-ray emitted from a source at the opposite side of the body and reconstruct a 3D attenuation map. Diagnoses based on CT is very popular, however an unnecessary exposure of X-ray must be minimal because of the damage to a human body. Furthermore, different aspects from different modalities such as MRI, PET, and SPECT [9] are required for medical diagnosis. Alternative technologies have therefore been developed over the years.

We focus on optical tomography, a modality of infrared light, in particular scattering tomography [4], [7]. Infrared light is safe to human body; devices can be small comprised of LEDs and chips, and less expensive than X-ray devices. A disadvantage is that light is scattered and diffused as well as attenuated inside a body, while X-ray is assumed not to be scattered. This problem makes the situation much more difficult. If no scattering, we would use a linear transform for this inverse problem like as the Radon transform for CT. Due to the scattering, a light path is no longer straight but rather complicated inside a body, and the observed light is not a sharp impulse but a blurred distribution of light.

There are two main approaches to the scattering tomography. One is Diffuse Optical Tomography (DOT) [3] which assumes that the light is extremely scattered inside the media. In other words, at each point of the media the light

scattering is modeled by isotropic diffusion. This process can be modeled by partial differential diffusion equations and solved by Finite Element Method. DOT has an advantage of the ability to trace how the light goes at each small time step (e.g. 10 pico seconds), however the diffusion assumption is often not adequate because infrared light of particular wavelength can penetrate human body with relatively small amount of scattering. The other approach is a tomography with single-scattering assumption [4]. If the media is optically thin and the scattering is quite low, then we can assume that the scattering event happens only once for each light path, i.e. single scattering is the dominant event. This assumption is opposite to that of DOT in which the dominant event is multiple scattering because the media is optically thick and scattering event happens so many times as the light travels through the media. Of course this single-scattering assumption is too strict to a variety of materials including human body.

Recently Ishii et al. [7] have proposed a scattering tomography for moderately scattered media, i.e., multiple forward scattering is dominant but diffusion is not. They assumed that the light is attenuated inside the material when the path of the light passes through a hidden object, which absorbs any light completely. To measure the attenuation due to the hidden object, they use a reference media in which there is no hidden object in order to compare the reference with the observed media. Obviously the use of reference is not practical in real situations, and hidden objects do not well model the distribution of attenuation inside real materials.

In this paper, we propose a multiple-scattering optical tomography without any reference to estimate the distribution of attenuation at each voxel in the material. As like Ishii et al. [7], we assume that multiple forward scattering events take place inside the media. We model the propagation of light through the media with thin layers: at each layer of the media, light is scattered from one layer to the next layer. This is a reasonable assumption because a layered model has been used for realistic human faces [10] and for anatomical description of human skin [11]. Also in the limit of infinitesimal thickness of layers, it can model continuous materials. In this paper we focus on 2D cases where the material is in 2D space divided into grid, however we can stack 2D materials to extend the method to 3D materials as described in [4], [7].

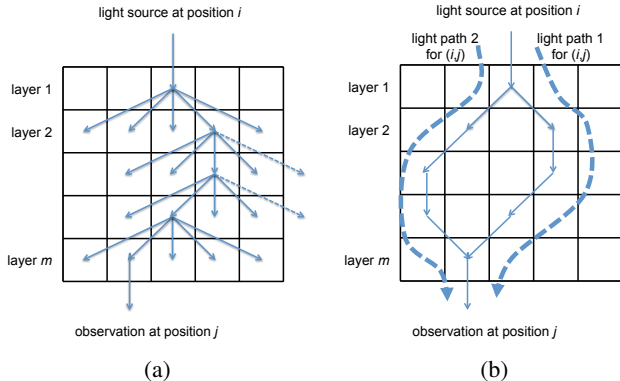


Figure 1: Scattering model of the layered material. (a) Layered model of a material. A light source at position i emits light to the first layer, then the light is scattered to the second layer. At the last m -th layer, output is observed at each position j . (b) Light scattering through layers. Even when the input and output positions (i, j) are fixed, there are multiple paths of light exist.

The rest of the paper is organized as follows. In section 2, we introduce our layers model of materials and scattering of light through the layers. An optimization based method to this scattering tomography problem is proposed in section 3. Experimental results with simulation and discussion of the proposed method is shown in section 4.

II. FORMULATION

In this section, we introduce our layered model of materials. Then we describe how light travels through the layers with scattering events. Finally we present an inverse problem to solve for tomography.

A. Layered material of 2D space

Our layered model is shown in Figure 1(a). A scattering material is assumed to be a 2D rectangle divided by m horizontal layers. Each layer is further divided into m voxels (therefore the material is a square grid in this case for simplicity of argument, but this can be changed). A light emitted from a light source goes to the first layer at position i ($i = 1, 2, \dots, m$) from the top side of the material. The light is scattered and attenuated at that voxel and distributed to the next layer, while some portion of light goes away from the material as shown in dotted arrow in Fig. 1(a). Once the light arrives to j -th voxel of m -th layer (the bottom layer), it is observed by a camera (detector) at position j . Incident and outgoing lights are assumed to be perpendicular to the layers.

This simple layered model of materials does not consider back scattering, therefore the light assumed to never go backward or sideways. Also the scattering event takes place only at the center of each voxel. As the light passes through a voxel, it is attenuated due to the absorption at each voxel.

Even if we fix the positions i, j of light source and observation, there are many possible light paths as shown in Figure 1(b). Therefore we use index k for a particular light path along with (i, j) . Because we assume that the material is divided into $m \times m$ grid, the number of possible paths for a given (i, j) pair is m^{m-2} , where -2 appears in the exponent to exclude the first and the last layers.

B. Scattering of light to the next layer

Scattering of light is extensively studied in physics [4], [12]–[15] for understanding the behavior of light as well as computer graphics [2], [6], [16]–[20] for rendering realistic images with participating media. We use however a very simple model of light scattering between layers of the material. A material affects on the light passing through the material in two ways: scattering and attenuation. We will describe these processes in this and next subsections.

Scattering is usually modeled by scattering coefficient (or scattering cross section) and a phase function. Scattering coefficients describe how often scattering events happen, and a phase function describes in which direction the light is likely to be scattered. Our simple model of scattering combines them into a single factor: we assume that the light at a certain voxel in one layer is scattered to another voxel in the next layer according to the distance between voxels. We model this process as a distribution of light from voxel i at layer n to voxel j at layer $n + 1$ and use the following Gaussian function:

$$p(\mathbf{x}_{n,i}, \mathbf{x}_{n+1,j}) = C \exp(-\|\mathbf{x}_{n,i} - \mathbf{x}_{n+1,j}\|^2 / \sigma^2), \quad (1)$$

where $\mathbf{x}_{n,i}$ is the coordinate of the center of voxel i at layer n in 2D space, C is a constant, and σ^2 is the variance that controls how light is scattered.

C. Attenuation of light along the path

Attenuation of light is due to absorption at each point in a material and also scattering away from the path along which the light would travel. This is usually modeled by the integral of extinction coefficients (the sum of absorption and scattering coefficients) along the path. We model this attenuation process as a finite sum instead of a continuous integral, and further an inner product of two vectors. We explain how we compute the attenuation by a finite sum first.

The intensity I_0 of a light emitted from a light source is attenuated as the light travels along a path k exponentially,

$$I_0 e^{-\int_k \sigma_t(\mathbf{x}) d\mathbf{x}}, \quad (2)$$

where σ_t is extinction coefficient at \mathbf{x} , and the integral is defined over the path k . In our model, the extinction coefficient is constant in each voxel because we divide the material into a grid. Hence this integral over a path can be transformed into the sum of the distance along a voxel multiplied by the extinction coefficient at that voxel.

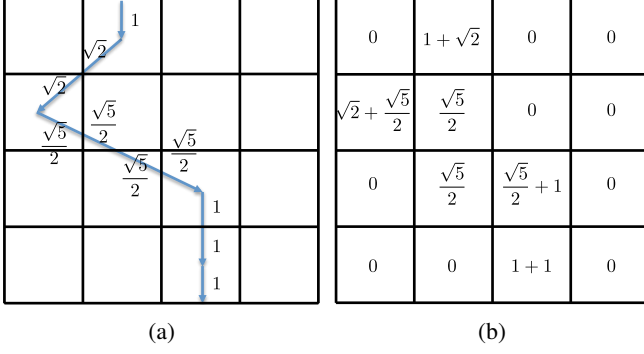


Figure 2: Example of light path and distances passing through each voxel. (a) Distances of each line segment are shown. Note that a voxel size is assumed 2×2 . (b) Distances of each voxel.

Figure 2(a) shows an example of a light path and corresponding distances that the path passes through each voxel. In this figure, distances of each line segment of the light path are shown. In this discretized material, the integral over the path can be computed by multiplying the distances (such as $1, \sqrt{2}, \frac{\sqrt{5}}{2}$ in the figure) by corresponding voxel extinction coefficient and taking the sum of them.

Further we write this summation as an inner product. Because line segments in the same voxel share the extinction coefficient at that voxel, the distances of those segments can be merged and stored in a grid as shown in Figure 2(b). Notice that the voxels through which the path does not pass have distance of 0. This enable us to represent the grid as a sparse vector. Let \mathbf{d} be a *distance* vector that is made by serializing the grid storing distances shown in Fig. 2(b) in the raster scan order (or whatever), and \mathbf{x}_e be a vector of extinction coefficients of the material serialized in the same order with \mathbf{d} . Then the summation can be simply written as the inner product of \mathbf{d} and \mathbf{x}_e , and Equation (2) can be written as

$$I_0 e^{-\int_k \sigma_t(\mathbf{x}) d\mathbf{x}} = I_0 \exp(-\mathbf{d}^T \mathbf{x}_e). \quad (3)$$

D. Observation model of scattered light

Now we can combine the discussions above to build an observation model of light. Let i be the position of incident light emitted from a light source and $i = 1, 2, \dots, m$ where m is the number of voxels in a layer (and also the number of layers), and j be the position of outgoing light observed by a camera. Light paths are indexed by k for a given (i, j) pair, hence a triple index i, j, k uniquely represent a single light path. A distance vector for a path i, j, k is represented by \mathbf{d}_{ijk} . Coefficients denoted by c_{ijk} is the product of scattering events of all layers:

$$c_{ijk} = \prod_{n=1}^{m-1} p(\mathbf{x}_{n,k_n}, \mathbf{x}_{n+1,k_{n+1}}), \quad (4)$$

where positions at each layer of the path i, j, k is $(k_1, k_2, \dots, k_{m-1}, k_m)$ and $k_1 = i, k_m = j$.

When we fixed the positions of incident and outgoing light positions to i and j , the observed light intensity I_{ij} is the sum of all contributions of possible paths of light,

$$I_{ij} = \sum_{k=1}^{m^{m-2}} I_0 \exp(-\mathbf{d}_{ijk}^T \mathbf{x}_e) c_{ijk}. \quad (5)$$

III. INVERSE PROBLEM

As we have derived the observation model of scattered light above, next we describe how to solve the proposed multiple scattering tomography as an inverse problem.

We have an equation (5) for a pair of (i, j) , that is, the positions of incident and outgoing points of light. Therefore we can vary these positions to obtain at most m^2 equations, which seem to enough to estimate m^2 number of unknown variables \mathbf{x}_e . What we want to do then is to solve the following optimization problem:

$$\min_{\mathbf{x}_e} \sum_{i=1}^m \sum_{j=1}^m |I_{ij} - \sum_{k=1}^{m^{m-2}} I_0 \exp(-\mathbf{d}_{ijk}^T \mathbf{x}_e) c_{ijk}|^2, \quad (6)$$

where c_{ijk} are given and hence scattering coefficients and a phase function are fixed since we have focused on the estimation of extinction coefficients at each voxel.

Extinction coefficients are positive by definition, therefore the optimization problem must be subject to constraints

$$0 \preceq \mathbf{x}_e, \quad (7)$$

where the symbol \preceq denotes generalized inequality that every elements in a vector must satisfy the inequality.

A voxel that completely block any light would have an extinction coefficient of the value infinity, which means the extinction coefficient has no upper bound. However, in terms of numerical stability, we found that a certain upper bound is preferable. Therefore, we add the following constraints as well:

$$\mathbf{x}_e \preceq u, \quad (8)$$

where $u > 0$ is a positive scalar.

This inequality constraint minimization problem can be solved by interior point methods. We have used the barrier method, an interior point algorithm, shown in Figure 3. We suggest that interested readers refer to [21] for further details. In short, the barrier method solves iteratively an unconstrained optimization problem by updating weight t that takes a balance between the original cost function and constraints. Each unconstrained minimization problem (9) is solved by the Newton's method in our implementation.

- 1: given a feasible initial solution \mathbf{x}_e , $t > 0$, $\mu > 1$, and $\epsilon > 0$.
- 2: **repeat**
- 3: $t \leftarrow \mu t$
- 4: solve the following minimization problem by starting from the current estimate:

$$\min_{\mathbf{x}_e} t f_0 - \sum_l (\log(x_{el}) + \log(u - x_{el})), \quad (9)$$

where f_0 is the original cost function (6), and x_{el} is the l -th element of \mathbf{x}_e . Update the estimation.

- 5: **until** $\frac{m'}{t} \geq \epsilon$, where $m' = 2m^2$ is the number of constraints.

Figure 3: An algorithm of the barrier method for solving our inequality constraint optimization problem.

IV. NUMERICAL SIMULATIONS

A. Simple material

We describe numerical simulation results of the proposed method for evaluation. A two-dimensional material is divided into 10×10 voxels as shown in Figure 4(a). The material has almost homogeneous extinction coefficients of value 0.05 except few voxels with much higher coefficients of 0.2, which means those voxels absorb light much more than other voxels. A light source is assumed to lit a light at each of m positions to the top layer, and a detector observes the outgoing light at each of m positions from the bottom layer. The variance σ^2 of Gaussian function (1) for scattering from one layer to the next layer is set to 2. The upper bound u in Eq. (8) is set to 1.

Estimated extinction coefficients are shown in Figure 4(b). The homogeneous part of the material with extinction coefficients of 0.05 (voxels shaded in light gray) is reasonably estimated because estimated values fall in the range between 0.04 to 0.06. In contrast, the dense part of the material with extinction coefficients of 0.2 (voxels shaded in dark gray) is not estimated well but looks blurred vertically. This blur effect is due to the experimental setting that the light paths go vertically from top to bottom inside the material.

This effect can be verified by simply rotating the setting by 90 degrees (now the configuration is a horizontal one) and applying the proposed method. Figure 4(c) shows the estimation result when the light source is on the left side of the material, and the detector is on the right side. The estimated extinction coefficients are blurred now horizontally because light paths go from left to right.

A simple trick to integrate these two results is to take the average of them, which is shown in Figure 4(d). The blur effect is then reduced by averaging and the estimation of extinction coefficients is improved. Root means square errors (RMSEs) for Fig. 4(b) and Fig. 4(c) are 2.92×10^{-4} and 4.40×10^{-4} , respectively. By averaging, RMSE for Fig.

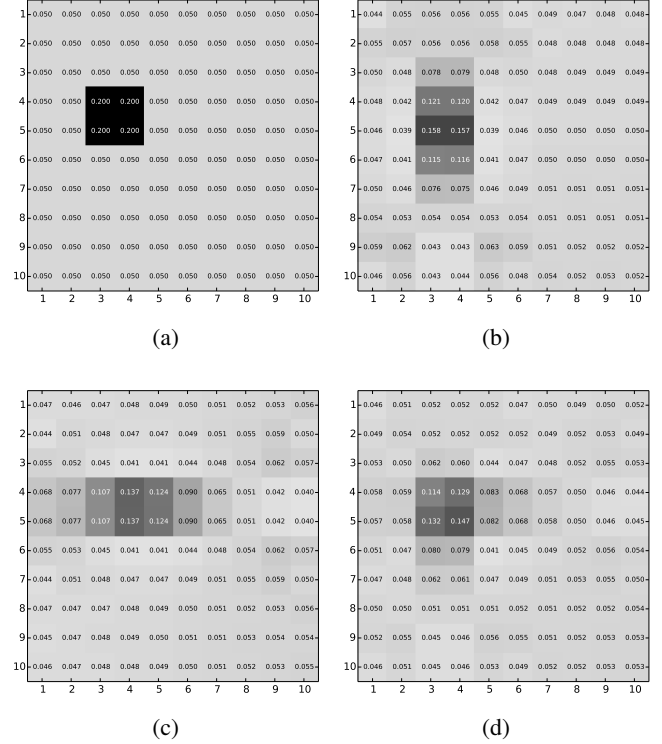


Figure 4: Simulation results of a material of size 10×10 . (a) Ground truth of the distribution of extinction coefficients shown as values in each voxel as well as by voxel colors. (b) Estimated extinction coefficients. A light source and detector are above and below the media. (c) Estimated extinction coefficients. A light source and detector are left and right sides of the media. (d) Average of (b) and (c).

4(d) decreases to 2.60×10^{-4} .

Values of cost functions are shown in Figure 6. The original cost function (6) decreases steadily and is less than 10^{-5} after 24 iterations, while the cost function of the barrier method seems not to change over iterations. These plots show that the barrier method effectively minimizes the original cost function while the constraints on the extinction coefficients are satisfied. This can be verified also as the observed and estimated light intensities as the difference of which is minimized. Figures 7(a) and 7(b) show observations I_{ij} for ground truth and estimation (of vertical configuration). Each row i in this matrix representation is a set of observations at j . For example, the third and fourth rows represent the observations where incident light position is $i = 3, 4$, where it is right above the dense voxels. Hence the observed light at $j = 3, 4$ below the dense voxels is much weaker than other diagonal values. Because our formulation of constraint optimization minimizes the difference between them, Figures 7(a) and 7(b) are quite similar to each other as the value of difference in Fig. 6 indicates.

Cost function values over iterations are shown in Figure

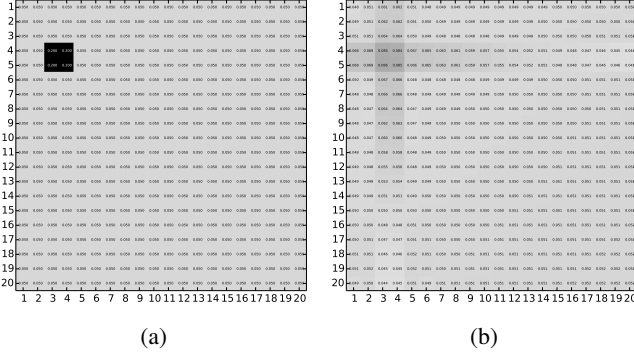


Figure 5: Simulation results of a material of size 20×20 . (a) Ground truth. (b) Estimated extinction coefficients by averaging.

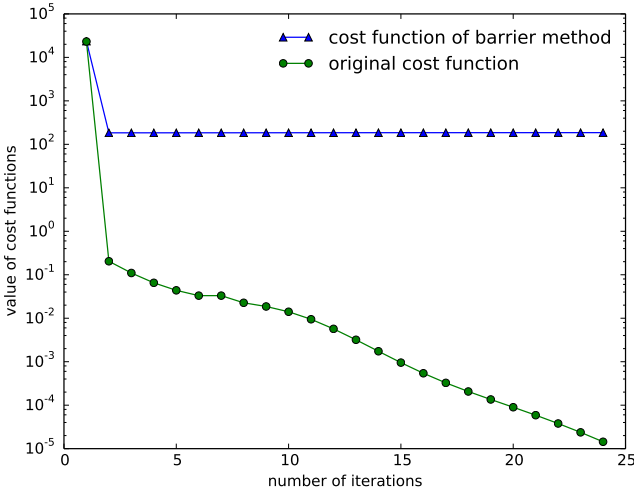


Figure 6: Cost function values over iterations for vertical configuration (a light source is above and a detector is below the material). The original cost function (6) is the residual between the model and observation, and the cost function of barrier method is that in Eq. (9) of Fig. 3.

9 for each material. These curves show that the proposed method effectively minimizes the objective function and seems to work well for any kind of materials.

For the material of 10×10 in Fig. 4(d), the proposed method takes about 2 minutes to converge (by MATLAB on a PC with Intel Xeon E5 2GHz). The most computationally expensive part is inverting the Hessian in the Newton's method. The computation time increases quickly; for 20×20 it takes more than two hours (a result is shown in Figure 5). We need an efficient implementation in the future.

B. Complex materials

Simulation results with more complex materials are shown in Figure 8. All materials are of size 10×10 but have more complex distribution of extinction coefficients. Estimated

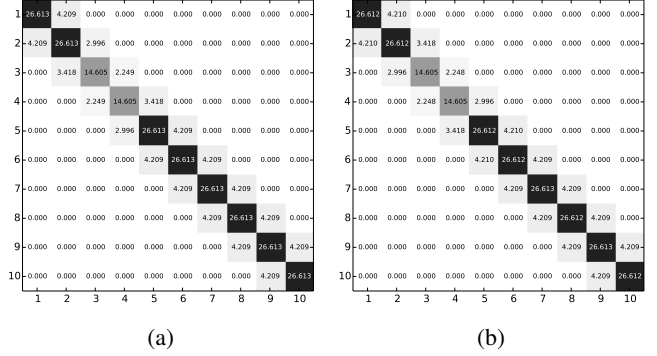


Figure 7: Observed light intensities $I_{i,j}$ of (a) ground truth and (e) the estimated material. For each position of light source i (which is the row index), a detector observes a set of light intensities shown as i -th row. The column index j represents the position of observation.

results are shown in the right column, made of the averaging results of vertical and horizontal configurations as in Fig. 4(d)

First material has four dense voxels apart from each other (Fig. 8(c)). Because vertically (or horizontally) aligned voxels affect to light paths, the estimated result has a significant blur effect that makes the appearance of the distribution a blurred faint rectangle instead of four corners (8(b)). This is a limitation of the proposed method currently, which must be improved in future.

Second material has dense voxels arranged in a U-shape (Figure 8(c)). Nevertheless this has also a lot of vertically or horizontally aligned voxels, the estimated result looks reasonable (Figure 8(d)) in which we can see clearly the U-shape is reconstructed. This result is quite promising, while the values of four corners are much thinner than the ground truth compared to voxels in between.

Third material mimics a phantom of a human body in which there are some dense voxels surrounded by less dense voxels, and those voxels are inside a round shape (Figure 8(e)). The estimated distribution shown in Figure 8(f) is, yet qualitatively, as good as we can see the distribution similar to the ground truth. Most voxel values estimated are smaller than the ground truth, however the distribution patterns of the ground truth and estimation are similar. The round shape with extinction coefficient of 0.05 in the ground truth can be also seen in the estimated result, while it is rather faint.

C. Reciprocity

One might think that the averaging four configurations gives a more better results, that is, we can add two configurations (bottom to top, right to left) in addition to the current two configurations (top to bottom, and left to right). Interestingly, the results of two vertical configurations (top to bottom and bottom to top) are exactly the same, and so

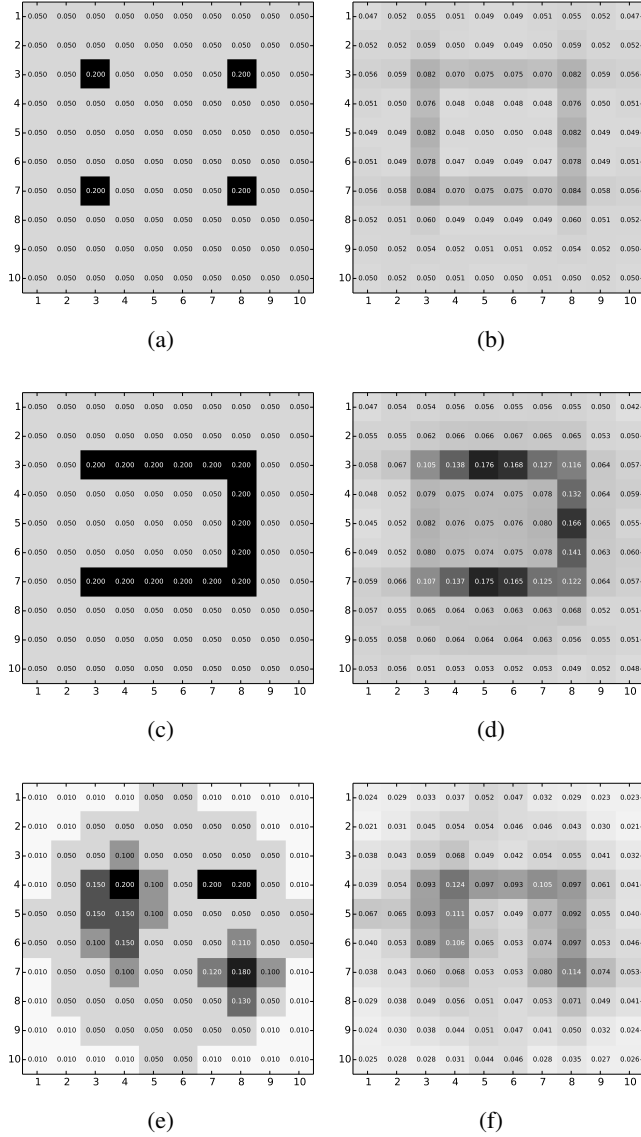


Figure 8: More simulation results of a material of size 10×10 . Ground truth distributions are shown in the left column and estimations are in the right column. (a-b) Four voxels have dense values. (c-d) Dense voxels are in a U-shape. (e-d) A phantom mimicking a human body.

are two horizontal two configurations (left to right and right to left). This has been verified by our preliminary results and also can be explained theoretically as follows.

The reason is that the formulation (6) has no direction information, where as we have explained the model as like it would be directed: a light goes the top layer from a light source above, passes through the media, then goes out and is observed by a detector below. The observation model (5) however simply describes how the light is attenuated when it goes along a particular path, and it does not matter which side is a light source or a detector. This *reciprocity* between

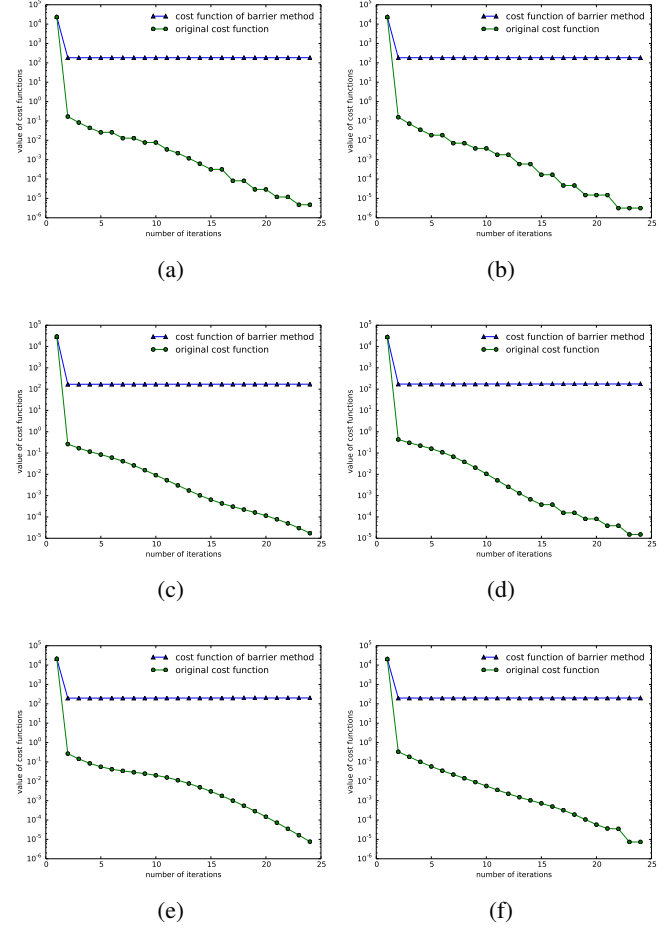


Figure 9: Cost function values for the materials of (a-b) four voxels, (c-d) U-shape, and (e-f) the phantom. Left column shows cost function values over iterations for the vertical configuration: a light source is above and a detector is below the material. Right columns shows for the horizontal configuration: a light source is left side and a detector is right side.

a light source and detector might be used for reducing the complexity of the problem, therefore we will explore it in future.

V. CONCLUSION

In this paper, we have proposed a method for multiple scattering optical tomography by assuming that the material is comprised of many layers and light is scattered layer by layer. Attenuation of light is modeled by an inner product of distance vectors, which represents how much a path passes through a particular voxel, and an unknown extinction coefficient vector. The inverse problem is formulated by an inequality constraint optimization problem that minimizes residuals between observed lights and predictions by the model, and then solved by an interior point method. Simulation results demonstrated that the proposed method

particularly works well for estimation of the distribution of extinction coefficients inside an inhomogeneous material.

Like as many previous works [4], [7], [13], currently we have evaluated the proposed method by numerical simulations with 2D materials. Our future work includes formulating vertical and horizontal configurations in to a single minimization problem, increasing resolution of a material with more voxels, incorporating more general scattering and non-rectangular media, evaluations with 3D materials and real materials, and dealing with interfaces between outside and inside the material.

ACKNOWLEDGMENT

This research is granted in part by the Japan Society for the Promotion of Science (JSPS) through the "Funding Program for Next Generation World-Leading Researchers (NEXT Program)" initiated by the Council for Science and Technology Policy (CSTP).

REFERENCES

- [1] S. R. Arridge, "Optical tomography in medical imaging," *Inverse Problems*, vol. 15, no. R41–93, 1999.
- [2] M. Pauly, T. Kollig, and A. Keller, "Metropolis light transport for participating media," in *Eurographics Workshop on Rendering Techniques*, 2000, pp. 11–22.
- [3] A. P. Gibson, J. C. Hebden, and S. R. Arridge, "Recent advances in diffuse optical imaging," *PHYSICS IN MEDICINE AND BIOLOGY*, vol. 50, pp. R1–R43, 2005.
- [4] L. Florescu, J. C. Schotland, and V. A. Markel, "Single-scattering optical tomography," *PHYSICAL REVIEW E*, vol. 79, pp. 036607–1–10, 2009.
- [5] Y. Dobashi, W. Iwasaki, A. Ono, T. Yamamoto, Y. Yue, and T. Nishita, "An inverse problem approach for automatically adjusting the parameters for rendering clouds using photographs," *ACM Transactions on Graphics*, vol. 31, no. 6, 2012.
- [6] C. Kulla and M. Fajardo, "Importance sampling techniques for path tracing in participating media," in *Eurographics Symposium on Rendering*, vol. 31, no. 4, 2012.
- [7] Y. Ishii, T. Arai, Y. Mukaigawa, J. Tagawa, and Y. Yagi, "Scattering tomography by monte carlo voting," in *IAPR International Conference on Machine Vision Applications*, 2013.
- [8] J. Hsieh, *Computed Tomography: Principles, Design, Artifacts, and Recent Advances*, 2nd ed. Wiley, 2009.
- [9] S. R. Cherry, "Multimodality imaging: Beyond pet/ct and spect/ct," *Seminars in Nuclear Medicine*, vol. 39, no. 5, pp. 348–353, 2009.
- [10] C. Donner and H. W. Jensen, "Light diffusion in multi-layered translucent materials," *ACM Transactions on Graphics*, vol. 24, no. 3, pp. 1032–1039, 2005.
- [11] T. Igarashi, K. Nishino, and S. K. Nayar, "The appearance of human skin: A survey," *Foundations and Trends® in Computer Graphics and Vision*, vol. 3, no. 1, 2007.
- [12] J. Wang, Z. Chi, and Y. Wang, "Analytic reconstruction of compton scattering tomography," *JOURNAL OF APPLIED PHYSICS*, vol. 86, no. 3, pp. 1693–1698, 1999.
- [13] W. Cong and G. Wang, "X-ray scattering tomography for biological applications," *Journal of X-Ray Science and Technology*, vol. 19, pp. 219–227, 2011.
- [14] P. González-Rodríguez and A. D. Kim, "Comparison of light scattering models for diffuse optical tomography," *Optics Express*, vol. 17, no. 1, pp. 8756–8774, 2009.
- [15] J. Heino, S. Arridge, J. Sikora, and E. Somersalo, "Anisotropic effects in highly scattering media," *PHYSICAL REVIEW E*, vol. 68, pp. 031908–1–8, 2003.
- [16] S. Premože, M. Ashikhmin, R. Ramamoorthi, and S. Nayar, "Practical rendering of multiple scattering effects in participating media," in *Eurographics Symposium on Rendering*, 2004.
- [17] M. Raab, D. Seibert, and A. Keller, "Unbiased global illumination with participating media," in *Monte Carlo and Quasi-Monte Carlo Methods 2006*, 2008, pp. 591–605.
- [18] M. Pharr and P. Hanrahan, "Monte carlo evaluation of non-linear scattering equations for subsurface reflection," in *SIGGRAPH '00*. ACM, 2000, pp. 75–84.
- [19] H. W. Jensen and P. H. Christensen, "Efficient simulation of light transport in scenes with participating media using photon maps," in *SIGGRAPH '98*. ACM, 1998, pp. 311–320.
- [20] Y. Yue, K. Iwasaki, B.-Y. Chen, Y. Dobashi, and T. Nishita, "Unbiased, adaptive stochastic sampling for rendering inhomogeneous participating media," *ACM Transactions on Graphics*, vol. 29, no. 6, December 2010.
- [21] S. Boyd and L. Vandenberghe, *Convex Optimization*. Cambridge University Press, 2004.